



The mirror blank is constructed as a thin meniscus type for an active mirror support in the telescope. The mirror prescription is shown in Table 1 and as it is described Figure 1 the aspheric departure is as large as approximately 9mm p-v.

Table 1. The prescription of the mirror

Items	Parameters
Material	Zerodur (SCHOTT)
Diameter (mm)	4200
Thickness (mm)	75 (aspect ratio=1/56)
Conic, K	-1
Radius of Curvature, RoC (mm)	16000
Off-axis Distance (mm)	4000
Aspheric Departure (mm)	9

Table 2 shows the fabrication specification and requirements of the mirror. The DKIST mirror specifically set a requirement for the Bidirectional Reflectance Distribution Function (BRDF) for the science.

Table 2. Specifications and requirements of the mirror

Items	Parameters
Surface Figure (nm RMS)	25
mid spatial figure (nm RMS)	8 (over 100~1mm)
Surface Roughness (nm RMS)	2
BRDF (sr <sup>-1</sup> )	1.0
Radius of Curvature, RoC (mm)	±15
Off-axis Distance (mm)	±2
Force Allowance, (N max)	20 (up to 30 modes)

Large aspheric departure makes the fabrication and testing difficult and the requirement for the high smoothness is another challenge. The details of fabrication and testing process have been described in the following sections.

## 2. METROLOGY SUPPORT

The mirror support is a critical element for the fabrication and metrology due to the extreme aspect ratio of the mirror blank construction. The mirror support of the telescope has 119 axial actuators with a set of force distribution to maintain the mirror shape. During the fabrication and testing the mirror is desired to be supported using the same set of force distribution as in the telescope. Additionally the long term stability over entire fabrication period is very important to ensure the high repeatability in metrology.

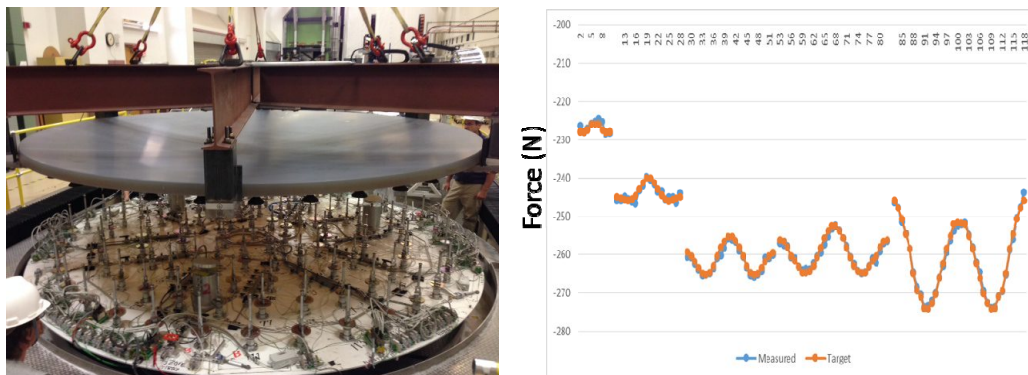


Figure 2. Mirror blank and metrology support (left) and targeted support force distribution and measured forces

As shown in Figure 2 fabricated mirror support provides very accurate force distribution less than 1N RMS, 4N p-v.

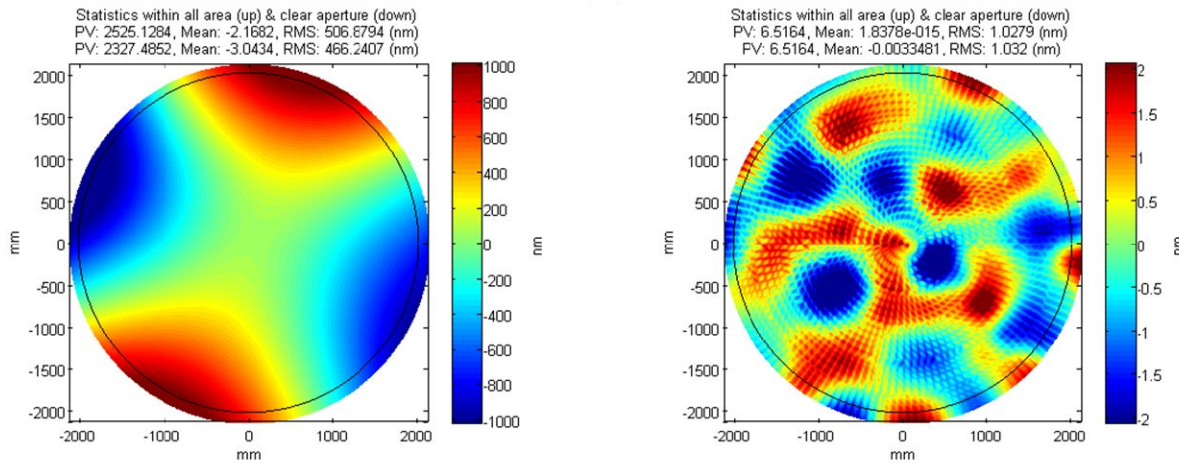


Figure 3. Mirror figure distortion due to support force error (Left) and residual after active correction (Right)

To evaluate the effect of the force difference between the target and measurement a finite element model is used. Using the model and measured force difference the surface figure is expected to be distorted as in Figure 3 in left and the residual figure after applying 30 bending mode correction is estimated as in Figure 3 in right. The residual surface and the correction force are 1nm RMS and 1N RMS respectively and both are well within tolerable range.

### 3. FABRICATION PROCESS

The mirror fabrication process is summarized in Table 3 from the generated blank to the final figuring. Metrology used for each processing phase is also listed with a redundant testing to ensure the result. All data processing and generating processing runs are done a custom optimization algorithm developed by the University of Arizona.

Table 3. Fabrication process of 4.2m off-axis primary mirror of DKIST

<ul style="list-style-type: none"> <li>• Generated Surface                             <ul style="list-style-type: none"> <li>– As delivered status: D64 Diamond Wheel</li> <li>– Inspection                                     <ul style="list-style-type: none"> <li>• Major dimension, Orientation registration, ROC</li> </ul> </li> </ul> </li> <li>• Rough Grinding                             <ul style="list-style-type: none"> <li>– Loose abrasive grinding with 40um Alumina</li> <li>– Various size passive Tools</li> <li>– Laser Tracker Surface Scan and Large Spherometer</li> </ul> </li> <li>• Fine Grinding                             <ul style="list-style-type: none"> <li>– Loose abrasive grinding with 25-12um Alumina</li> <li>– Various size passive tools</li> <li>– IR SCOTS surface measurement and Laser Tracker</li> </ul> </li> <li>• Polish out                             <ul style="list-style-type: none"> <li>– Cerium Oxide polishing</li> <li>– Active stressed lap and Passive tools</li> <li>– SCOTS surface measurement and Laser Tracker</li> </ul> </li> <li>• Figuring                             <ul style="list-style-type: none"> <li>– Cerium Oxide polishing</li> <li>– Various size passive tools</li> <li>– SCOTS and CGH Null Interferometry</li> </ul> </li> </ul>
--

Computer Controlled Fabrication system has been used for entire DKIST mirror processing. Newly developed multi-axis fabrication system with 600 mm active Stressed lap and 300mm passive FLEX lap are shown in Figure 4. The multi-axis computer controlled fabrication system has features of generating orbital and spinning motion and also real time feedback of the local position of the tool in the mirror coordinate. The Stressed lap is designed with 12 active bending actuators to conform the lap surface to fit to the local aspheric surface of the mirror. The passive FLEX lap is designed and optimized to the mirror figure to maximize the smoothing and figuring effect.

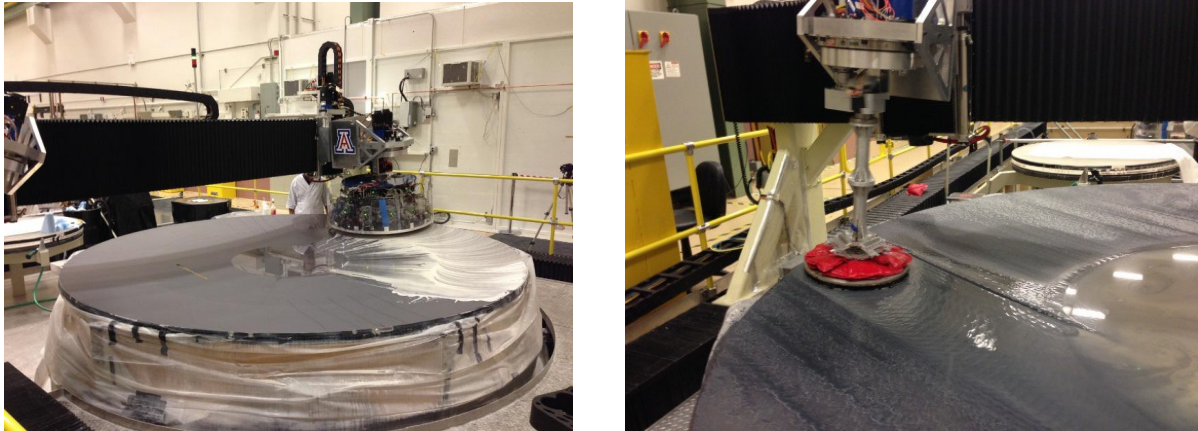


Figure 4. 600mm Active Stressed lap (Left) and 300mm FLEX lap (Right)

The fabrication schedule and convergence chart is shown in Figure 5. The total duration of the fabrication took about 13months from the generated blank until the completion of fabrication. Thanks to the computer controlled fabrication system and well planned metrology, it was very efficient process.

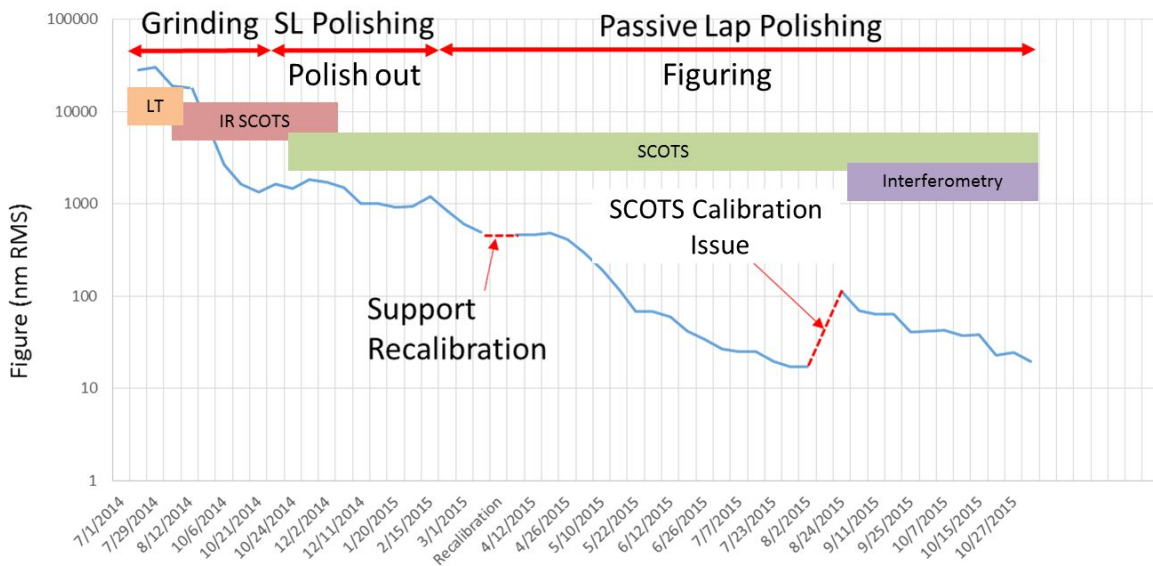


Figure 5. Fabrication schedule and convergence of DKIST primary mirror

A photo of finished DKIST primary mirror on the metrology support is shown in Figure 6. The multi-axis computer controlled fabrication system is also shown in behind of the mirror.

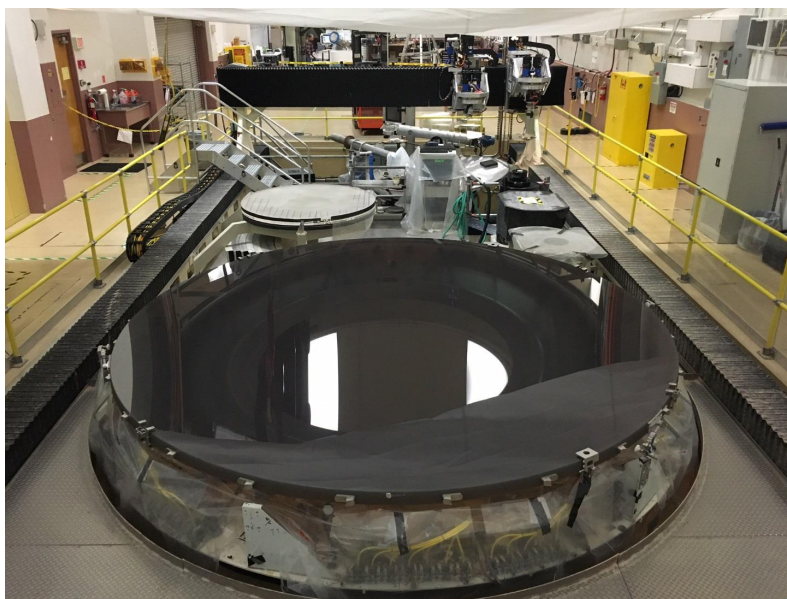


Figure 6. Photo of finished DKIST primary mirror

#### 4. METROLOGY

The surface figure metrology is planned to cover the required spatial range covering the full aperture, mid spatial frequency feature and surface finish. Additionally BRDF requirement is set to specify the scattering.

For the full aperture surface metrology CGH null interferometry is performed for the principal test and Visible SCOTS test is used to guide fabrication as well as a redundant test. Figure 7 shows error budget of the principal optical test.

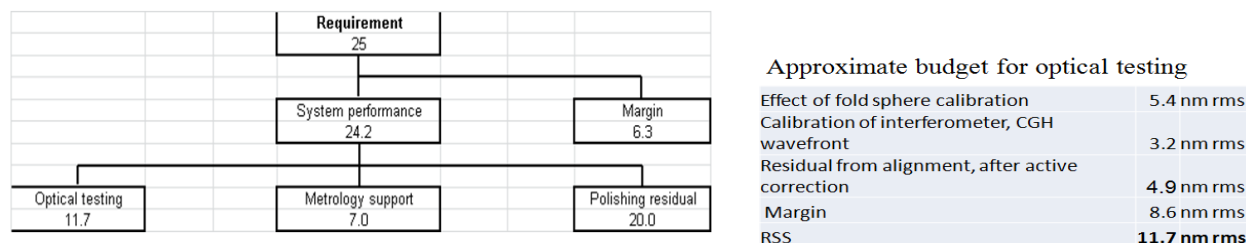


Figure 7. Surface metrology error budget

Subaperture deflectometry and micro finish topography are used to evaluate mid-spatial frequency feature and surface finish. The details of metrology have been discussed in the following sections.

##### 4.1 Visible Deflectometry – SCOTS

The SCOTS technique works for measuring aspheric optics without requiring additional optics. We illustrate the dynamic range of the technique using the reverse ray trace interpretation of the test where the camera aperture is replaced with a point source. The reflected light from this point source from the aspheric mirror under test would intercept the display and create an illumination pattern. The size of the display must be large enough to accommodate all of the ray bundles as defined by this reverse ray trace. If the display can be located near the center of curvature, then this

size is approximately equal to twice the product of the aspheric slope (the gradient of the aspheric departure) and the radius of curvature.<sup>3,4</sup>

For SCOTS test of DKIST primary mirror, two cameras and one large LCD display are configured as in Figure 8 at near the center of curvature. The display was selected to illuminate the mirror with phase shifting. Two camera provides simultaneous deflected image acquisition. SCOTS test has been performed 8 different positions of the mirror. With the configuration total of 16 measurements were made and averaged.

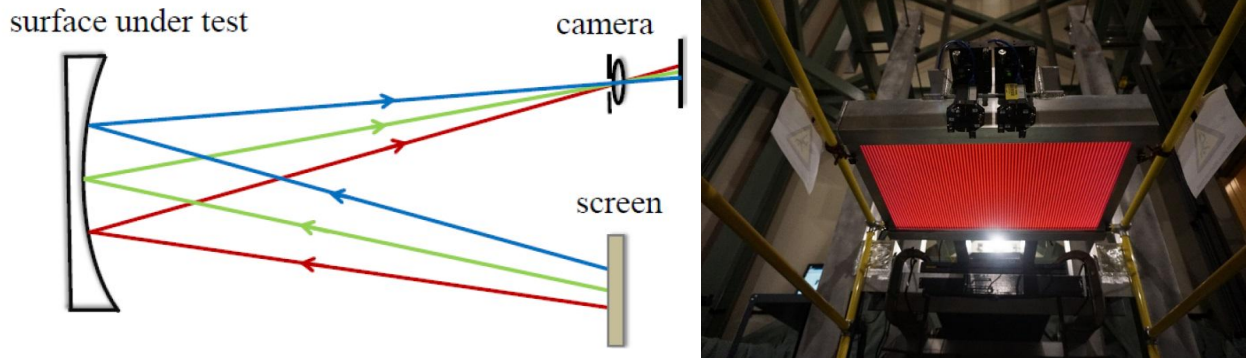


Figure 8. Concept of SCOTS test (Left) and actual SCOTS test configuration of DKIST primary mirror (Right)

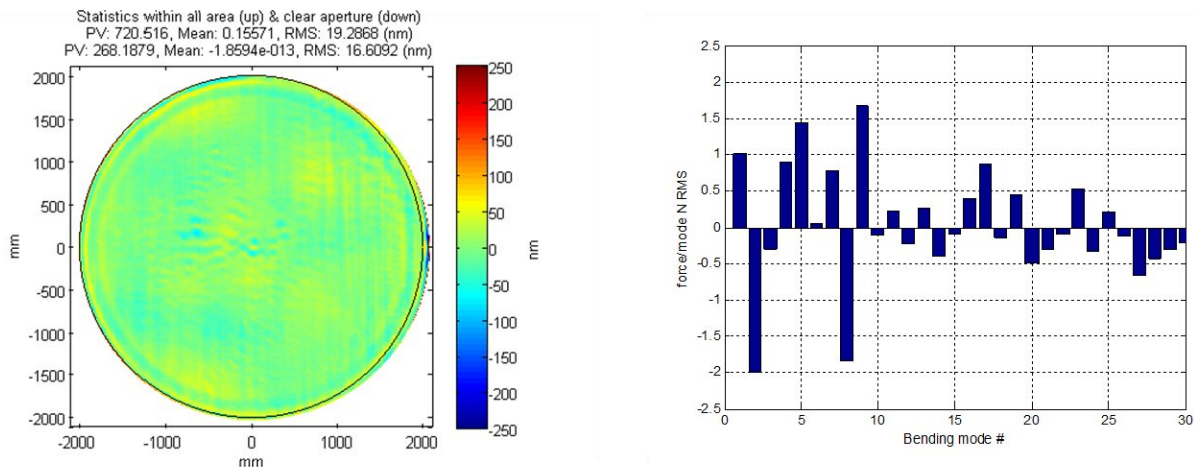


Figure 9. Surface measurement (Left) and modal correction force (right) from Visible SCOTS

The final result from Visible SCOTS test is presented in Figure 9.

#### 4.2 IR Deflectometry<sup>3,5</sup>

The SCOTS technique requires specular reflection from the surface, and we desire measurements of ground glass surfaces that are diffuse for visible wavelength light. We achieve these measurements by utilizing a longer wavelength that reflects from these rough surfaces. We use thermal infrared radiation from a heated tungsten filament as the source, and a thermal imager that uses a microbolometer array as the camera. We call this system SLOTS, the Scanning Longwave Optical Test System. We performed measurements to evaluate the reflectivity of a thermal source as a function of grit size for the grinding of the surface. We get adequate reflectance for fine ground surfaces made using loose abrasives as large as 25  $\mu\text{m}$ .

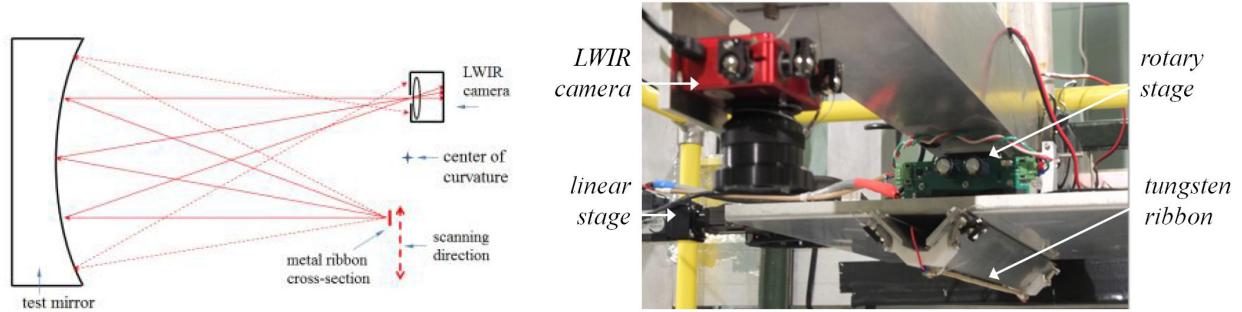


Figure 10. Concept of IR SCOTS test (Left) and actual SCOTS test configuration of DKIST primary mirror (Right)

The IR SCOTS test was very efficient metrology to guide the mirror fabrication process down to approximately  $1 \mu\text{m}$  RMS surface with 25-12  $\mu\text{m}$  grit loose abrasive grinding.

#### 4.3 Principal Metrology – CGH Null Interferometry

The interferometry approach for DKIST primary mirror is similar to optical testing performed on two other large mirrors – primary mirrors of NST and GMT - fabricated at the University of Arizona. A layout of the null test is in Figure 11. A large fold sphere is used to compensate for most of the astigmatism generated by testing the off-axis primary mirror at its center of curvature. The residual aberration is corrected using a computer generated hologram (CGH). Careful alignment and calibration of these components is required.

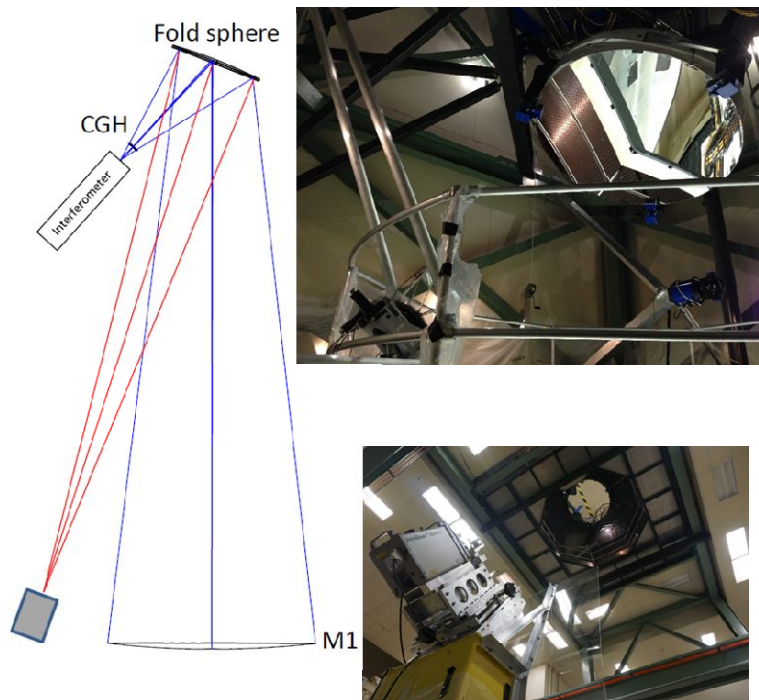


Figure 11. Construction of the interferometry

The tolerances established for the test are shown in Table 4. The Interferometer Assembly (IA) consists of a 4D PhaseCam 6000 Interferometer and the CGH. Critical alignments are measured using a FARO laser tracker. Sphere Mounted Retroreflectors (SMRs) for the tracker measurements are attached to the CGH, large fold sphere, and the primary mirror (the latter on removable fixtures placed at the four compass points)..

Table 4. Alignment tolerance of the CGH null interferometry of DKIST

Parameter	Tolerance
CGH to Interferometer Tilts	1/3 Fringes
CGH to Interferometer Focus	1/4 Fringes
IA Decenters (X, Y)	50 $\mu\text{m}$
IA Focus (Z)	50 $\mu\text{m}$
IA Tilt(X), Tilt(Y)	0.001 $^\circ$
IA Tilt(Z)	0.01 $^\circ$
Large Fold Sphere Tilts	0.0014 $^\circ$
Large Fold Sphere Defocus	30 $\mu\text{m}$
Primary Mirror Tilts	5 Fringes

The large fold sphere is a 1.8 m mirror mounted to a hexapod. An ESDI Intellium H2000 interferometer was mounted at the center of curvature of this mirror, providing a measurement of its figure error that is subtracted from the measurement of the primary. SMRs are mounted directly to the mirror surface, allowing use of a laser tracker to accurately align the mirror using its hexapod.

The 9" CGH contains the null pattern, an alignment pattern, fiducial patterns, small Fresnel lens patterns, and a chrome patch as in Figure 12. The alignment pattern is an annular zone whose fringes are used to align the CGH to the interferometer. The fiducial patterns project spots onto the edges of the primary mirror, along the symmetry axis. The small Fresnel Zone Plate patterns are used to accurately align SMRs that are bonded to the CGH surface. The diameter of the CGH provides an insufficient baseline for the laser tracker to support the 0.001 $^\circ$  tilt tolerance on the CGH. This tolerance is achieved using the reflective chrome patch to measure the mirror image of an SMR.

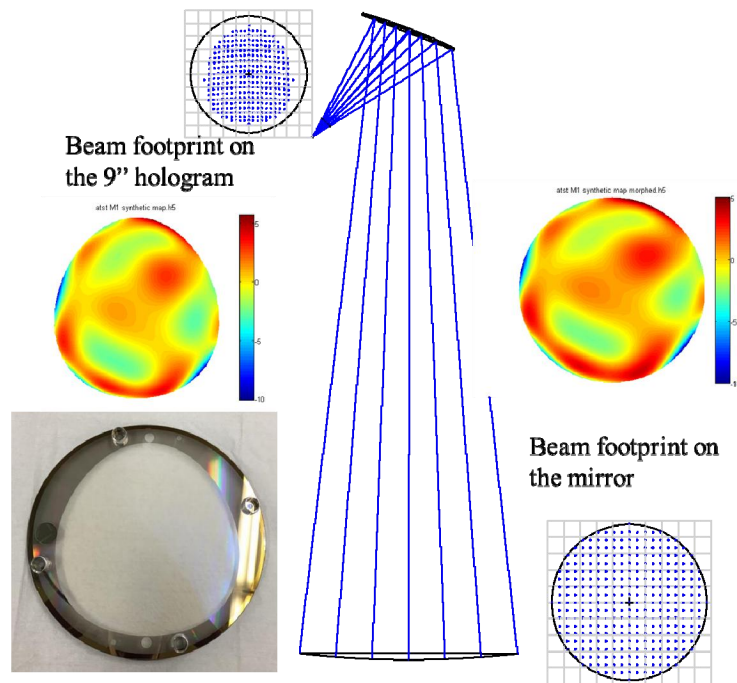


Figure 12. Surface figure distortion and Computer Generated Hologram (CGH)

The test configuration puts significant mapping distortion into the beam as shown in Figure 12. This must be removed to create an accurate surface map in coordinates on the primary mirror, as well as for subtracting errors from the large fold sphere from the primary interferometer measurement. We use orthogonal mapping polynomials to morph the maps. Fiducials are placed on the primary mirror and measured using a laser tracker. The 4D interferometer measurement is morphed into the primary mirror coordinates using data from a ZEMAX ray trace.

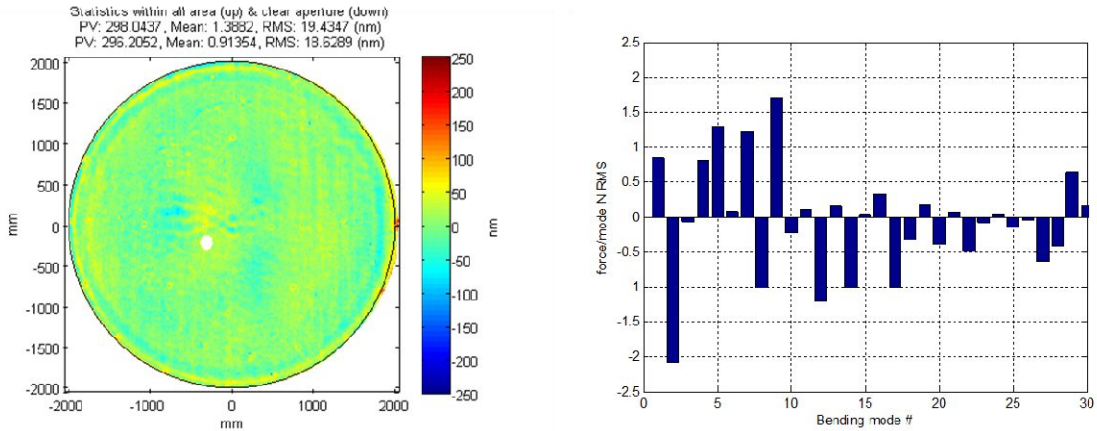


Figure 13. Surface measurement (Left) and modal correction force (right) from CGH null interferometry

The final measurement from CGH null interferometry of DKIST primary mirror is shown in Figure 13.

#### 4.4 Subaperture Deflectometry - SPOTS

SPOTS is a portable SCOTS system that uses a micro-display and collimating lens that can be set on top of a large mirror to measure high frequency surface irregularities from 10 to 1000 cycles/m. The layout of the test system is shown below. This system measures to sub-nm precision over a 125 mm diameter region. The dynamic range provides the ability to measure aspheric surfaces, which gives SPOTS a distinct advantage over interferometry. Also, this system can be refocused to measure surfaces with wide range of curvatures from concave through flat to convex.<sup>3</sup>

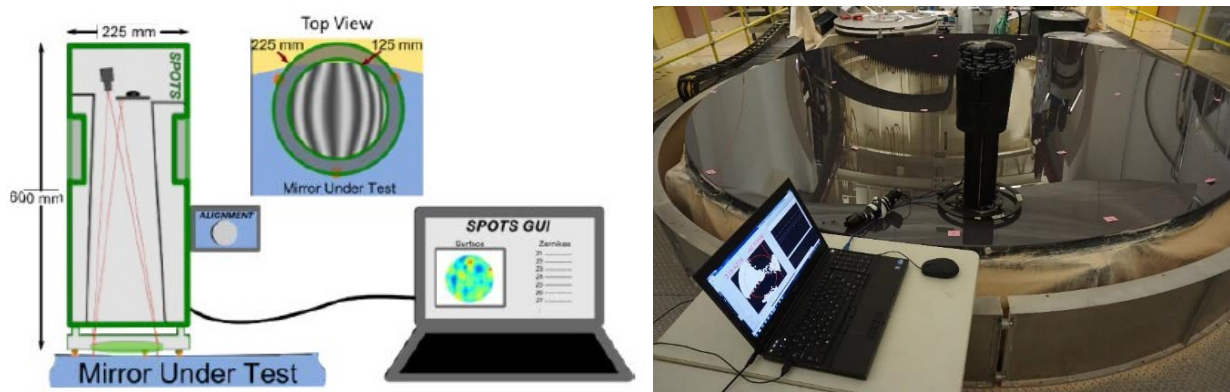


Figure 14. System configuration of SPOTS (Left) and photo of SPOTS measurement on the DKIST mirror

The actual test configuration and photo taken from the measurement are shown in Figure 14. The measured data are presented in Figure 15 and the result shows 3.6-5.2 nm RMS over 125 mm circular aperture.

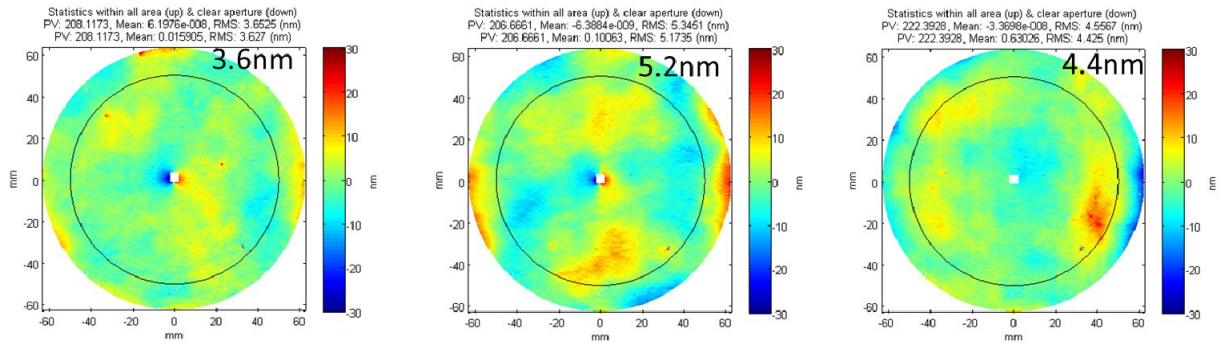


Figure 15. SPOTS measurements of DKIST mirror

#### 4.5 Surface Finish and BRDF

The surface finish of DKIST primary mirror has been evaluated by measuring the surface roughness using the Micro Surface Topography (MFT) apparatus as in Figure 16. With 2.5x Nikon Mirau objective and 1024x764 pixel camera the measurement covers approximately 3mm x 2.5mm rectangular aperture with 3  $\mu\text{m}$  spatial resolution. The measured surface roughness was approximately 1nm RMS as in Figure 17.

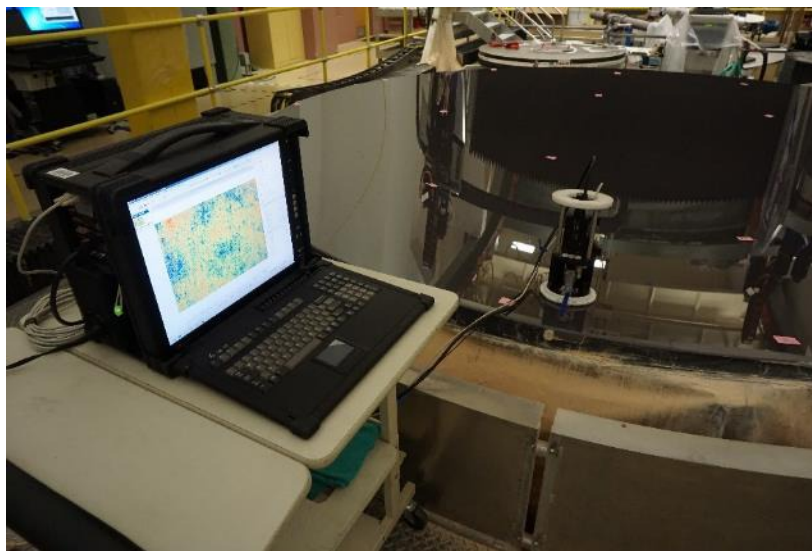


Figure 16. Photo of surface finish measurement using Micro Finish Topography apparatus

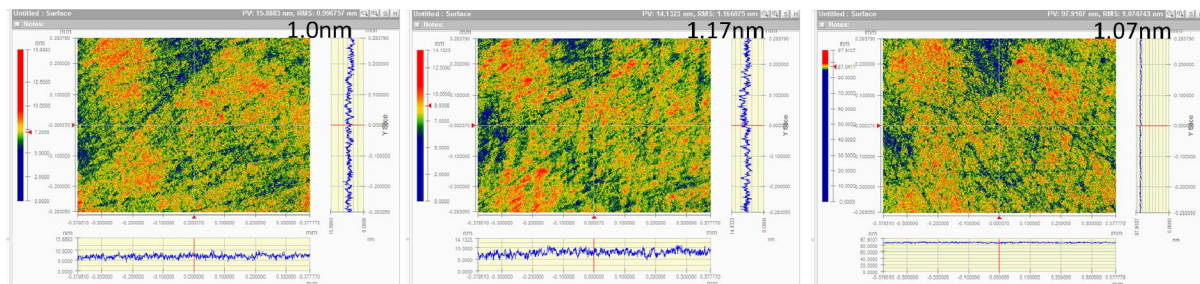


Figure 17. Surface finish measurements

In addition to the surface roughness, the requirement for Bidirectional Reflectance Distribution Function (BRDF) was specifically set for the mirror. The BRDF of the finished DKIST mirror was evaluated using PSD by converting BRDF using Rayleigh-Rice theory.<sup>6</sup> As in Figure 18 the measured BRDF meeting specification very well.

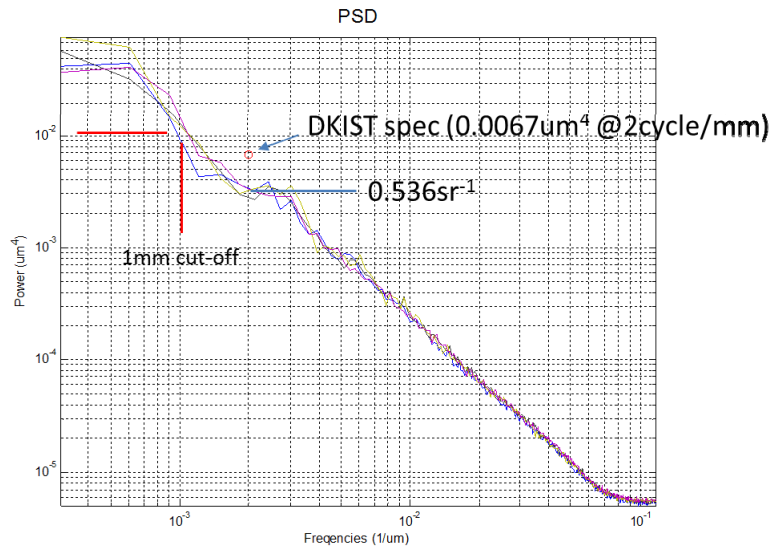


Figure 18. Power Spectrum Density (PSD) plot with BRDF specification and performance

## 5. CONCLUDING REMARKS

Fabrication of the 4.2m off-axis aspheric primary mirror of DKIST has been successfully completed and the summary of the finished mirror performance is shown in the Table 4. The mirror meets every aspect of the specification and requirement. UA team finished the mirror to 10 Angstrom roughness. Typical mirrors are finished with 20 Angstrom and this causes a small amount of scatter, which shows up as glare. With this “Super Polished” surface meets very specific BRDF(scatter) requirement. Maybe, no other large optics have been made to such precision.

Table 4. Summary of fabrication performance of 4.2m off-axis primary mirror of DKIST

Items	Requirement	Delivered value
Radius of curvature for off-axis paraboloid (OAP)	16000 ± 15 mm	16000 ± 0.08 mm
Off axis distance with respect to ideal OAP	4000 ± 2 mm	4000 ± 0.18 mm
Clocking angle with respect to ideal OAP	< 2 arcmin	0 ± 0.052 arcmin
Surface irregularity over full aperture	< 25 nm rms	< 18.8 nm rms
High frequency surface errors (1 – 100 mm period)	< 8 nm rms	5.14 ± 1.2 nm rms
Surface roughness (< 1 mm period)	> 20 Å rms	10.5 ± 1.1 Å rms
BRDF at 0.002 radians from specular	< 1.0 sr <sup>-1</sup>	0.568 ± 0.193 sr <sup>-1</sup>
Combined area for all surface imperfections	< 200 mm <sup>2</sup>	58.9 mm <sup>2</sup>
Maximum actuator force required for active correction	< 20 N	10.9 N
Clear aperture diameter projected onto off axis mirror	4.000 m	4.000m

## 6. ACKNOWLEDGEMENTS

We thank to DKIST primary mirror fabrication project team including Dr. Chen Liang and Dr. Joseph McMullin in NSO and also thank to Optical Engineering and Fabrication Facility at College of Optical Sciences including Mr. Jeffrey Kingsley, Mr. Bruce Cook, Mr. Daniel Caywood, Mr. Logan Graves and many others who supported the project behind the scenes.

## REFERENCES

- [1] J. P. McMullin et al., “The Advanced Technology Solar Telescope: design and early construction,” Proc. SPIE 8444, 844407 (2012).
- [2] National Solar Observatory, [Advanced Technology Solar Telescope], ([http://dkist.nso.edu/sites/atst.nso.edu/files/press/ATST\\_book.pdf](http://dkist.nso.edu/sites/atst.nso.edu/files/press/ATST_book.pdf)), 2014
- [3] J. H. Burge, P. Su, G. Butel, R. Huang, A. Maldonado, T. Su, “Measuring large mirrors using SCOTS, the Software Configurable Optical Test System”, Proc. SPIE 9151, (2014)
- [4] Tianquan Su, Won Hyun Park, Robert E. Parks, Peng Su, James H. Burge, “Scanning Long-wave Optical Test System – a new ground optical surface slope test system”, Proc. SPIE 8126, (2011).
- [5] Peng Su, Manal Khreishi, Run Huang, Tianquan Su, and James H. Burge, “Precision aspheric optics testing with SCOTS: a deflectometry approach”, Proc. SPIE 8788, (2013).
- [6] Kashmira Tayabaly, John C. Stover, Robert E. Parks, Matthew Dubin, James H. Burge, “Use of the surface PSD and incident angle adjustments to investigate near specular scatter from smooth surfaces”, Proc. SPIE 8838, Optical Manufacturing and Testing X, 883805 (September 7, 2013); doi:10.1117/12.2024612.